GreenMO: Flexible and Virtualized Green Communications Architecture

Paper # 563

Abstract

With the turn of new decade, wireless communications face a big challenge on connecting more and more new users and devices, at the same time being energy efficient and minimizing its carbon footprint. However, the current approaches to keep up with data rates while adding more users either end up demanding new spectrum resources, as is the case with OFDMA, or demanding a lot of power consumption in the RF front end processing chains, as is the case with Massive MIMO. GreenMO addresses this dichotomy by creating a new multi-user communications architecture which is both spectrum- and power-efficient. That is, GreenMO brings about an order of magnitude power savings by reducing to power consumption to $O(1)$ from the current $O(N_{\text{ant}})$ in the current Massive MIMO architectures having N_{ant} antennas. The key insight GreenMO has, to optimize the power consumption, is introduction of virtualization of the RF chain hardware . That is, instead of using multiple physically laid RF chains, GreenMO creates these RF chains virtually on the fly, being flexible to the user load. Thus, GreenMO paves for green& flexible communication architectures. We prototype GreenMO on a PCB with eight antennas and evaluate it with a WARPv3 SDR platform in an office environment. The results demonstrate that GreenMO is 3× more power-efficient than traditional Massive MIMO and 4× more spectrum-efficient than traditional FDMA systems, while multiplexing 4 users.

1 Introduction

Current wireless systems have a very high carbon footprint of 1.4% , close to aviation industry that has a footprint of 2%. So, the wireless industry is aiming to reduce this footprint by 45% by 2030, by optimizing for energy consumption [1, 2]. This is going to be a gargantuan task even with advancements in efficient radio designs, with billions of more devices getting connected [3] and increasing data rate trends [4]. Thus the wireless systems, more specifically, the next generation base-stations will face a challenging time reducing energy footprint to meet the target, while keeping up with data rates to add new users/devices. Hence, the need of the hour is to develop base-stations that are ideal or green i.e., figure out a way to add users and maintaining data rates for each user, (1) while optimizing for both spectrum and power (2) being flexible and Scale-able, so the energy consumption is proportional to the amount of data communicated.

To achieve a green communication system, a straight forward way for base-stations to keep up is by adding new spectrum to support more users and maintaining data-rate and leverage radio design enhancements in sub-6 GHz to reduce energy consumption[1]. However spectrum is scarce in sub-6 GHz, and expensive and needs to be utilized in an efficient way [5, 6]. For example, in WiFi6's OFDMA [7] the increasing users are served by slicing the fixed aggregate spectrum into multiple slices that serve each user, providing each user a narrow slice of non-interfering channel. While, this makes the AP need constant energy to process the fixed number of users, it would lead to low-data rates per user, which defeats the purpose of spectrum efficiency.

To overcome the limited spectrum per user, there is an increasing trend towards Massive MIMO systems for serving large number of users (let's say N) concurrently over entire spectrum by deploying larger antenna arrays ($N_{\text{ant}} > N$) on the base station and create spatially non-interfering channels to serve each user, thus providing spectrum efficiency [8–13]. However, these multi-antenna (N_{ant}) Massive MIMO arrays results in extreme energy in-efficiency and lacks flexibility. First, massive MIMO would in turn require N_{ant} individual (radio) RF front end processing chains (RF-chains), which would increase the overall power consumption by N_{ant}× [14–17]. Additionally, an ideal green system should only need to perform computation and typically backhaul only N data-streams for serving N users. However, the Massive MIMO system would need to backhaul and compute on $N_{ant} >> N$ data streams for serving N users. Finally, the backhaul and compute of the data, doesn't reduce even if the number of users are reduced in the system (as reduced antennas lead to loosing the degree of freedom). Thus, the additional N_{ant} backhualing ends up using compute power inefficiently.

An ideal green communication system should be most power efficient, where all the power consumption is proportional to amount of data moved across the system. Next, the green communication system should minimize the power consumption of the RF-chains to be minimal and constant (or $O(1)$), instead of on the orders of the number of users (or $O(N)$ for N users). Taking a step towards realization of the green communication system, in this paper we present GreenMO, which meets all these stringent requirements by developing a system which utilizes just a single RF front-end chain (constant $O(1)$ RF front end power consumption), at the same time supporting data-rate of N users communicating simultaneously on the entire spectrum concurrently. By supporting N users, we mean it can enable N non-interfering channels over the entire spectrum. Furthermore, GreenMO achieves green communication system, where it can serve N users on entire spectrum, with just N× sampling+compute

[1] mmwave and THz spectrum tend to be not reliable i.e. easily blocked by blockage and mobility

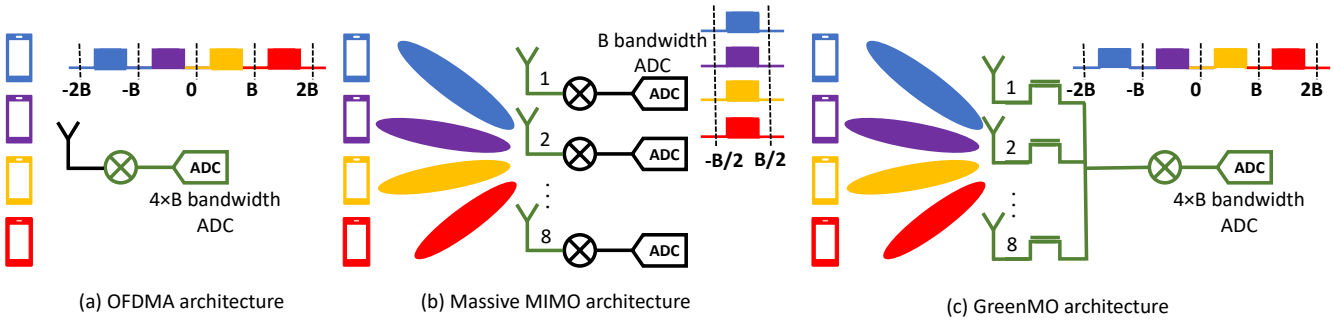

(a) OFDMA architecture (b) Massive MIMO architecture (c) GreenMO architecture

Figure 1: GreenMO puts forward best of both worlds: (a) As power efficient as OFDMA and (b) as spectrum efficient as Massive MIMO

power, which can not be reduced further to avoid info-theoretic implications. That is we cannot get more data rate without getting more digital samples processed. Furthermore, GreenMO is flexible, i.e. with decreasing users the compute and sampling is reduced proportionally as well, thus maintaining constant power consumption with decreasing users.

The first key challenge for GreenMO is to achieve (constant $O(1)$ RF front end power consumption) while supporting the massive MIMO architecture. The key-insight which allows GreenMO to come up with a single RF chain design is the amalgamation of the concepts of OFDMA with that of massive MIMO. Intuitively, it maps different spatial directions/users on the spectrum to non-overlapping frequencies very much like OFDMA. More accurately, GreenMO creates N virtual RF chains from a single physical RF chain's sampled at appropriate $N\times$ bandwidth to deliver the spectral efficiency of massive MIMO (Fig. 1(b)) while enjoying power benefits of OFDMA's single physical RF-chain design (Fig. 1(a)). Fundamentally, as shown in Fig. 1(c) if antennas are receiving a signal of B bandwidth spectrum, GreenMO's intuition is to fit N antenna signals of B bandwidth each across the NB sampled single RF chain. It is important to note here that the over the air spectrum received by the antenna is of bandwidth B and the net sampled bandwidth is NB. We thus enable N virtual RF-chain creation by providing N distinct frequency shifts to each antenna's RF-signal such that they occupy different parts of the sampled NB bandwidth.

No we need to figure out how one can provide these N distinct frequency shifts across N antennas without consuming $O(N)$ the power to justify our $O(1)$ RF front end power claim. To do this, GreenMO inspires from backscatter communication's RF-switches that create frequency shifts to signals [18–22], with minimal to no additional power requirements. Thus with NB sampled bandwidth, we can create N different phase frequency shifts of B bandwidth each, such that each antenna's signal has a discernable frequency shift. This enables GreenMO to recover the N antenna signals from the NB sampled single RF chain, allowing capability to handle N users with just $O(1)$ RF front end power.

Additionally, this intuitive design choice of employing RF switches combined with configurable sampling rate to virtualize the concept of an RF chain, makes GreenMO a highly flexible architecture. Thus, by varying the sampling and switching frequencies of the architecture, GreenMO can increase/decrease the number of RF chains on the fly, allowing GreenMO to flexibly adjust to the user conditions. That is, unlike existing Fig. 1(c) solutions if the user load decreases, GreenMO can automatically reduce the number of RF chains to flexibly meet the new demands.

So far we have discussed how GreenMO gets one antenna stream per virtual RF chain. But, with N antennas and N virtual RF chains we can not serve N users in a robust manner. A naive solution here would be to do $N_{\text{ant}} > N$ antennas and create N_{ant} virtual RF chains, so that we can borrow from massive MIMO solutions employing this many physical RF chains, to robustly serve N users. Although this satisfies $O(1)$ spectrum requirements and nearly $O(1)$ front end consumption, it will have ($N_{\text{ant}}\times$) compute+sampling. Here, instead GreenMO generalizes our virtual RF chains, where a virtual RF chain can utilize or connect or combine to one or more antennas. Thus, GreenMO uses the generalized concept to create only N virtual RF chains to serve N users, but still continuing to leverage ($N_{\text{ant}} > N$) antennas. Thus achieving both spatial diversity of ($N_{\text{ant}} > N$) and the compute power requirements of $O(N)$.

To perform the mapping of antennas to virtual RF chains, GreenMO designs an algorithm which we refer to as 'Binarized Analog Beamforming (BABF)' to enable this virtual hybrid beamforming with simple $0-1$ RF switches. The key idea is that, GreenMO uses N_{ant} antennas per virtual RF chains, to beamform towards one user per virtual RF chain, instead of isolating per-antenna signals via the virtual RF chain. In BABF, we strategically switch the antennas to *beamform to one user per RF chain, instead of one antenna per RF chain.* Thus we show that we can serve N same frequency band users with N_{ant} antennas and N virtual RF chains. GreenMO architecture to do so demands only $O(1)$ spectrum, $O(1)$ RF front end power and $O(N)$ compute+sampling power, being

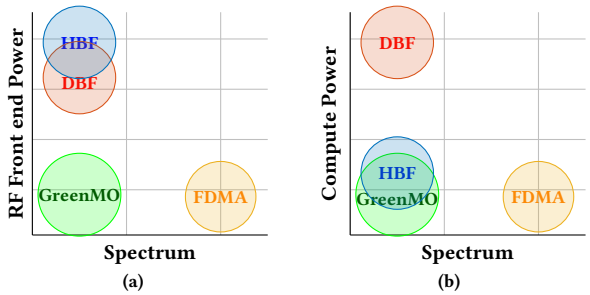

Figure 2: Power and Spectrum efficiency comparison: (a) RF front end power compared vs spectrum efficiency (b) Compute Power vs Spectrum Efficiency. Showing how GreenMO is the most optimal.

the first green architecture which can keep up with the power and spectrum efficiency requirements of the new decade.

Thus, to summarize, GreenMO designs a new beamforming architecture which utilizes a single RF chain to create many virtual RF chains, and show that this flexible architecture can be green and drastically cut down both on RF front end power as well as sampling+compute power. We implement and test our antenna array prototype with WARPv3 SDR and 802.11 OFDM waveforms with 4 users, over multiple user positions in a conference room setting, as well as digital beamforming and FDMA baselines. Our key results include similar performance metrics with digital beamforming with 3× less power requirements, achieving the same network capacity as compared to FDMA with 4× lesser spectrum requirements, and $>$ 10 dB improvement in 90 percentile performance for average SINR across the 4 users over traditional architectures.

2 Background and Motivation

Recall that our goal is to achieve next-generation green communications which are spectrum-efficient. The current gold-standard for spectrum-efficiency communications is Massive MIMO, and therefore in this section, we would review the state-of-art massive MIMO architectures and put them in perspective with green communications. The key idea behind massive MIMO is to use massive number of antennas N_{ant} as compared to the number of users N so to capture enough degrees of freedom required to create N spatial streams. In that context, there are two popular multi-antenna architectures, digital beamforming and hybrid beamforming. To understand how green these architectures are, we study these in two aspects of power consumption in wireless transceivers while maintaining spectral efficiency: (1) radio front-ends and (2) the sampling and compute for decoding.

2.1 Energy Consumption for radio front-ends

Most popular architecture in sub-6 GHz is digital beamforming architecture (DBF) [8–13]. DBF basically connects each of the N_{ant} antennas to radio frontend processing chains (RF chains), which downconvert the signals received by the antennae and get it ready for digital baseband sampling. The goal of DBF here is to procure the antenna's degrees of freedom at the digital baseband level, where signal processing can then create N non-interfering spatial streams, one for each user.

Features	FDMA	DBF	HBF	GreenMO
Spectrum Req.	O(N)	$O(1)$	O(1)	$O(1)$
RFE Pow.	$O(1)$	$O(N_{ant})$	$\sim O(N_{ant})$	$O(1)$
Compute Pow.	$O(N)$	$O(N_{ant})$	$O(N)$	$O(N)$
Sampling Pow.	$O(N)$	$O(N_{ant})$	$O(N)$	$O(N)$
Flexibility	Yes	Yes	No	Yes

Table 1: Comparison of GreenMO with existing techniques

This specific design of RF front end design makes the digital beamforming inefficient in its power consumption at the front-end. The reason behind this power inefficiency is that amongst the various analog components in the RF chain, the dominant power consuming operation is the downconversion of each N_{ant} signals. This downconversion for each antenna needs high quality LO signal distributed, which is extremely power hungry and a challenging process. Primary reason for this is that the quality of LO degrades as you split the signal power of the LO [9, 23, 24], and therefore the architecture needs active low-noise amplification circuits to distribute the LO. Furthermore, these split LO's for Massive MIMO operations need to be phase synchronized with very low phase noise, which makes the process more power hungry [9, 25]. The end result of this complex LO distribution to serve N users is that it dominates the power consumption, making the DBF's front end design constantly drawing watts of power for its spectrally efficient operations.

On the otherhand, there are Hybrid beamforming (HBF) approaches that try to reduce the RF front end power consumption by using analog pre-processing networks which constructs only N outputs one for each user instead of $N_{\text{ant}} > N$ [14–16, 26–34]. These N outputs are then downconverted to decode the user data. These analog pre-processing networks are typically a network of phase shifters. These phase shifters are configured such that it projects the N_{ant} degrees of freedom available at the RF front end to well conditioned N degrees of freedom at digital baseband. This analog phase configuration establishes N spatial streams without requiring downconversion of additional $N_{\text{ant}} - N$ streams However, these phase shifters still require N physical RF-chains, so that the power hungry LO distribution is still existing (albeit reduced by a factor of N_{ant}/N). An additional point to note is that this analog phase shifting network has very high insertion losses (about 10dB) [9, 17, 27]. These insertion losses need to be compensated for via increased power consumption from the power-amplifiers. Often this additional power requirement from the amplifiers offsets the power savings at the RF front end due to reduction of RF chains from N_{ant} to N. Thus making the HBF RF front end almost as power hungry as DBF as shown in Fig. 2b.

Thus, we can see that both DBF and HBF consume power on the order of the number of antennas ($O(N_{\text{Ant}})$). But we know that, RF front end power consumption is a constant power requirement just to set up the hardware, and it should not scale upward with the number of antennas required for massive MIMO. Thus, true requirements of a green communications architecture, should be to cut this RF front end power consumption to the lowest of limits, by making it a constant ($O(1)$) instead.

2.2 Energy consumption for sampling and compute

In addition to the RF front end power consumption of multi-antenna architectures, it is also important for green architectures to consider the power consumption for digital sampling, and the data backhauling+compute power thereoff. However, unlike RF front end power, this is not a fixed power consumption cost due to hardware, and depends on the user load. Thus, the challenge to optimize this power consumption is different than that of front end. That is for a truly green architecture we need to *flexibly* adjust the sampling and the compute power consumption to always be order of number of users, $O(N)$.

Unfortunately DBF needs to backhaul and compute N_{ant} antenna streams at the digital signal processor to obtain the N interference free per-user streams. Thus, this makes DBF further inefficient, as it deals with compute+sampling of N_{ant} streams in addition to exacerbated power requirements already. On the other hand, the hybrid architectures reduce the RF-chains fromN_{ant} to N via analog circuits and feedback only N streams to efficiently use sample and compute. However, HBF today is a fixed architecture which optimizes compute+sampling only for N users. Since ideally the compute power should scale with N, it can not be optimized for a fixed number of users. That is, if the number of users increase/decrease, HBF can not arbitarily scale to higher/lower RF chains required since the architecture relies heavily on the fixed laid down phase shifter network.

In summary, requirements from a truly green architecture are two-fold with respect to power consumption: (1) Have O(1) power consumption at the RF front ends to minimize the setup power costs and (2) Have O(N) power consumption for sampling+compute to minimize the running power costs, flexibly in response to the corresponding N users' load. In addition, the green architecture needs to meet (1) and (2) while maintaining the spectrum efficiency, i.e., all the N users need to share the same existing spectrum resource.

3 Design

To achieve the two-fold requirements for a green architecture set in section 2, GreenMO aims to develop next generation Base Stations that optimize for both the setup power costs at the RF front-end and running power costs of sampling+compute. In this section, we first dive into the idea of how GreenMO's architecture drastically cuts down on the RF front end power costs in section 3.1. Then we show how GreenMO optimizes the running costs by minimizing the sampled data, and data backhauling+compute thereof in section 3.2. We further ensure that GreenMO's optimization for power in both RF front end and data backhauling+compute does not compromise the spectral efficiency. Finally, we also show in these sections that the GreenMO's current design enables it to be flexible and scalable with increasing/decreasing number of users in the environment.

3.1 GreenMO's solution to optimize RF front end power

GreenMO first aims to design an extremely power efficient RF front end. Power efficiency at the RF front end would imply sever requirements, i.e., we need an architecture that draws only constant power in the RF front-end irrespective of the number of users being served by the base station. The reason for this constant RF front end power consumption requirement, is because this power consumption is a operational power for the architecture. This power will be consumed no matter how the user load varies, since it is associated with just setting up of the physical hardware being used by the architecture. Thus, GreenMO has to figure out how to have constant power consumption at the base station's RF front end for varying user load.

While the current spectrum efficient systems like Massive MIMO, are not power efficient as their power consumption is proportional to the number of RF-chains laid down, which at best is loosely proportional to the maximum number of users (N) they intend to serve. So the fixed power these architectures consumed thus is $O(N)$. Typically these architectures are designed for maximum number of users, N_{max} and then irrespective of the active user load the architecture experiences, the architectures will keep on guzzling $O(N_{max})$ power, thus not being green at all. Thus the key design principle which GreenMO overcomes these shortcomings is by laying just one single physical RF-chain connecting all the antennas, making the power consumption to $O(1)$, a constant minimal power consumption.

A natural question at this stage is how does GreenMO get back the required degrees of freedom if GreenMO uses multiple antennas connected to a single RF chain? The key insight that helps GreenMO to overcome this limitation is by borrowing the frequency division concepts from OFDMA. TO be more precise, recall that in order to serve N, B bandwidth users, OFDMA would widen the sampled bandwidth to NB and have the N users in N different non-intefering frequency bands. What if GreenMO could do the same, but

with antennas instead of users? That is, sample $N\times$ more bandwidth, and try to fit each individual signal of N antennas into non-interfering frequency bands across the NB sampled bandwidth.

At first glance, it may seem that we are trading off the front-end power consumption to the sampling power consumption, by using NB bandwidth to get N antenna signals. However, this is not the case. The reason is that ADC's power scales linearly with frequency[9, 17], with the ADC power equation being

$$P_{ADC} = \text{FoM} \times F_s \times 2^q$$

where FoM is a constant referred to as figure of merit, F_s is sampling frequency and q is the quantization bits used in ADC. What we are proposing here is to replace the traditionally used N different ADCs sampling at B each, with a single ADC sampling at NB. Due to linearity of ADC power consumption with sampling frequency, power consumption of NB ADC will be the same as N different B ADCs.

Henceforth, GreenMO's first design principle is to have multiple antennas connected to a single ADC, which will be sampling at $N\times$ rate to capture N RF chains abstracted over the sampled bandwidth. We refer to this concept of creating RF chains over the ADC's digitized samples as 'virtual RF chain' creation, since in a way, we virtualize the concept of emulating many virtual RF chains created from a single high-speed physical RF chain. What virtualization gives us is a design which works with just a single downconnversion chain, which meets the $O(1)$ power requirements. In addition, we get flexibility on adaptively increasing/decreasing number of RF chains by just tweaking the ADC's sampling rate, leading to a flexible design. A natural question at this point would be, how does GreenMO actually enable this virtual RF chain creation? That is, how does GreenMO guarantee that antennas' signal can be accomodated across the NB sampled ADC bandwidth, so that GreenMO can create these virtual RF chains?

Toy example to show virtual RF chain creation

To explain the concept of virtual RF chain creation, let us consider a simple toy example, where we have a 2 antenna, antenna array. As an abstraction, consider first antenna receives a triangular signal and the second antenna receives a rectangular pulsed signal, both signals in frequency domain having bandwidth B. Today's way of capturing the 2 degrees of freedom offered by the array by massive MIMO is to have 2 physically laid RF chains, which downconvert and sample these rectangular and triangular signals directly (Fig. 3(a)).

On the other hand, Fig. 3(b) shows a naive attempt at replacing multiple RF chains in Fig. 3(a) by virtualizing the chains over a single physically laid RF chain, however, by merely increasing the ADC rate. This leads to combining of the signals from the antennas before getting downconverted by the RF chain, which gives a raised triangular signal in

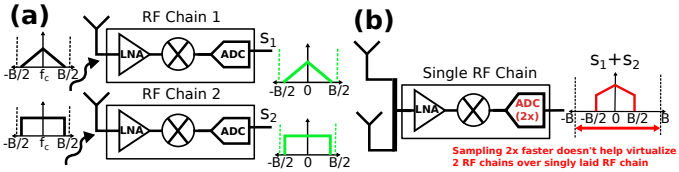

Figure 3: Toy example showing (a) 2 physical RF chains and (b) a naive approach towards virtualization by increasing merely the ADC sampling rate

this scenario. Since the antenna signals have got combined, 3(b) fails to create these 2 virtual RF chains with isolated triangular and rectangular signals in them. Thus, merely increasing ADC rate does not by itself create these virtual RF chains, as by increasing the ADC sampling rate we actually did not get any new information on how to untangle the combined antenna signals. This is because there is just noise and no antenna signals in the additional spectrum captured by the ADC, when it's sampling rate is doubled in hopes of creating 2 virtual RF chains.

The key concept behind GreenMO architecture is to create useful signal copies in the neighbour bands, instead of just noise as compared to the naive example considered before. That is create copies of useful signal in the additionally sampled bands, so that when ADC sampling rate increases to accomodate virtual RF chains, it gets the capability to untangle the combined antenna signals to successfully create the virtual RF chains. To create these signal copies, we need to somehow shift the antenna signals to neighbour bands, before the signals get downconverted through the RF chain. Additionally, we also need to create these signal copies in a low-power fashion to stay true to the requirements of a power-efficient architecture.

To do that, GreenMO's insight here is to augment the antenna array with RF switches (Fig. 4) toggling with *on-off* codes having time period, equal to signal bandwidth to perform this frequency shifting. Similar toggling RF switches have also been used for backscatter communications [18–22], which also demand low-power operation. These RF switches in backscatter applications create frequency shifts in reflected signal to avoid interference with line of sight signal. Similarly, GreenMO uses these low-power RF switches to create frequency shifts of the RF signals before they get downconverted. Now that we have these frequency shifts of the antenna signals, the higher sampling rate ADC will be useful as it will capture different frequency shifted antenna signals instead of just neighbour band noise.

So, in order to create these virtual RF chains over a singly laid physical RF chain, GreenMO uses strategic toggling of the RF switches, combined with ADCs increased sampling rate. To understand this strategic toggling logic, without loss of generality let us revisit the aforementioned toy example of 2 virtual RF chains and it can easily be extended to creation of N RF chains that is discussed later. So, for the 2 antenna toy

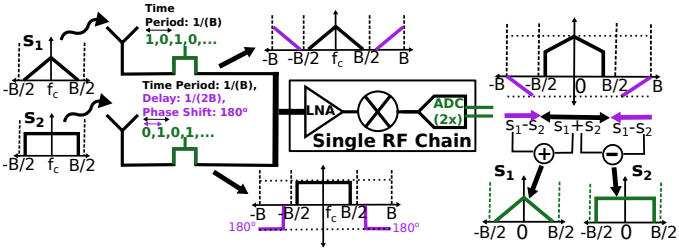

Figure 4: Toy example demonstrating GreenMO's approach to create virtual RF chain from one physically laid chain

example, when GreenMO wants to create 2 virtual RF chains, the ADCs would be sampling at $2B$, where B is the signal bandwidth, to accommodate the 2 signals from each RF chain. Thus, a single ADC sample will occupy total time of $\frac{1}{2B}$, and in order to shift the signals by frequency B, the switching code has to repeat every 2 ADC samples. This presents us two possible codes $0, 1, 0, 1, 0, 1, \ldots$ and $1, 0, 1, 0, 1, 0, \ldots$. When we supply these codes to one of the 2 antennas, we have one antenna being toggled *on* for odd samples, and the other antenna toggled *on* for even samples.

This strategic toggling actually creates sum of the 2 antenna signals in the first Nyquist band ($(-B/2) < f < (B/2)$) and difference of the 2 antenna signals in the second band ($(-B) < f < (-B/2)$ and $(B/2) < f < (B)$), as shown in Fig. 4. The reason is that $0, 1, 0, 1, 0, 1, \ldots$ and $1, 0, 1, 0, 1, 0, \ldots$ are basically π shifted versions of the same frequency codes, and hence the frequency shifted copies they create will reflect this π shift, leading to creation of subtracted signals in second band. Fundamentally, this then allows us to separate the per-antenna signals by simple signal processing, first add the signals extracted from each Nyquist band and then take the difference as illustrated in Fig. 4. Thus GreenMO creates these virtual RF chains with a single physically laid RF chain and strategically toggles the multiple switches connected to the multiple antennas to serve multiple users in a low-power and spectrum efficient fashion.

To further provide some mathematical intuition on why this effect happens, say the antenna signals were $s_1(t), s_2(t)$, these signals are B bandwidth. The codes $c_1 = 0, 1, 0, 1, \ldots$ $c_2 = 1, 0, 1, 0, \ldots$ are basically 50% duty cycled codes with frequency B, and RF switches implement these codes in RF domain before downconversion and ADC sampling. Thus, the ADC finally samples the waveform $s_1(t)c_1(t) + s_2(t)c_2(t)$, at $2B$. In addition to a constant DC component, these switches also produce harmonics at $\pm B$. Since the codes have a frequency B, thus time period $\frac{1}{B}$, and the associated time delay between c_1, c_2 is $0.5(\frac{1}{B})$, thus the phase associated with this time delay would be $(\frac{2\pi}{\frac{1}{B}})0.5(\frac{1}{B}) = \pi$.

Thus, as shown in Fig. 4 the frequency domain view of the signal sampled by ADC, would have a summed up signal $(0.5 * (s_1(t) + s_2(t)))$ in the first Nyquist band, $(-\frac{B}{2} < f < \frac{B}{2})$ and a differential signal $(0.5 * (s_1(t) - s_2(t)))$ in the second Nyquist band, $((-B < f < -\frac{B}{2}) \cup (\frac{B}{2} < f < B))$. A simple digital processing step can now get us back s_1, s_2 by simply adding the subtracting these signals in the two Nyquist bands.

Hence, GreenMO utilizes RF switches with different phase codes, coupled with an increased sampling rate ADC in order to virtualize the RF chains. This design effectively marries OFDMA to massive MIMO, we end up using more sampling bandwidth to create virtual RF chains over frequency, which allows GreenMO to be as spectrum efficient as massive MIMO and as power efficient as OFDMA.

Generalization to N antennas:
The method of obtaining these virtual RF chains from a single physically laid chain can be easily generalized when we have N antennas with N RF switches and an ADC which is doing $N * B$ times sampling where B is the signal bandwidth. In this generalized scenario, we will now have N codes $c_1, c_2 \ldots c_n$, which will be codes of length N with $c_1 = 1, 0, 0, \ldots, 0, 0$, $c_2 = 0, 1, 0, \ldots, 0, 0, \ldots$, $c_{N-1} = 0, 0, 0, \ldots, 1, 0$ and $c_N = 0, 0, 0, \ldots, 0, 1$. Since these codes are $1/N$ duty cycled they will have frequency images at every integral multiple of B and thus total N images at frequencies fftshift$(0, B, 2B, \ldots (N-1)B)$. In addition to these frequency images, each code c_i is delayed by $\frac{(i-1)}{NB}$, and thus the j-th harmonic of c_i will have a phase of $\frac{(i-1)}{NB} * \frac{2\pi}{\frac{1}{jB}} = (i-1) * j * \frac{2\pi}{N}$. We can then implement a similar signal processing algorithms as the 2-antenna toy example to extract each individual antenna's user signal.

The reason this generalization works out is because all these are different series of roots of unity, and by doing phase inversion one set of the roots become all co-phased and thus their virtual RF chain component adds up, and the other sets of roots still remain phase shifted versions of their previous versions and add up to 0, which allows GreenMO to extract the RF chain per antenna from the increased sample rate ADC stream. A more formal mathematical formulation of the N antenna generalization can be found in Appendix 8.1.

Using virtual RF chains for spatial-multiplexing:
Once we are able to obtain the per-antenna waveforms $\mathbf{S} = [s_1(t), s_2(t), \cdots, s_N(t)]^T$, the process to obtain the spatially multiplexed output is straightforward and follows the same method as compared to usual way with physically laid RF chains. In the scenario when we have N antennas and N RF chains, and say we have N users, we can perform MIMO channel estimation with the N virtual RF chains to get the $N \times N$ channel matrix for all N users and N antennas.

Now, we can choose any precoding strategy to suppress the signals from other users to get individual streams for each of the N users. For example if we use a simple ZF precoding would multiply the $N \times N$ matrix $\mathbf{H}^{-1}$ to the obtained virtual RF chain matrix $\mathbf{S}$ to get individual interference free N_s

samples of each N-th users data, stored in the $N \times N_s$ matrix $\mathbf{U} = \mathbf{H}^{-1}\mathbf{S}$. We choose to implement only the linear precoding schemes, like MMSE, BD or ZF, since these schemes, in particular, ZF have been experimentally verified to meet the system capacities [8], while the non-linear precoding methods like THP are still under theoretical research.

Thus, by using just 1 physically laid RF chain, GreenMO creates N virtual RF chains with N antennas and N RF switches, while only $O(1)$ RF front end power consumption.

3.2 GreenMO's solution to optimize sampling+compute power

Now that we have seen how GreenMO designs to optimize for the power consumption on the RF front end to be limited to $O(1)$ in section 3.1. Let us now dive into understanding on how should GreenMO's architecture be designed so as to handle the N antenna's sampled data that needs to backhauled and computed, which adds additional power constraints on the base station.

A key thing to note is that so far in section 3.1, we have assumed that the N users interfering can be resolved by the degrees of freedom provided by the N antennas connected to these N virtual RF chains. Unfortunately, in practical scenarios, it is infeasible to serve N users interfering with just N antennas. The reason is that the channel matrix $\mathbf{H}$ often ends up being non-invertible and ill-conditioned to support N spatial stream generation [28, 30, 35]. Today's massive MIMO architectures, both digital beamforming and hybrid beamforming, use $N_{\text{ant}} > N$ antennas in order to serve N users in a robust manner. The reasoning behind the $N_{\text{ant}} > N$ antennas requirement is to capture more than enough degrees of freedom to allow creation of robust N spatial streams, one for each user.

However, to optimize for sampling+compute power it is required to have only N data streams to serve N users and at the same time use N_{ant} antennas. Thus, in order to optimize for sampling power GreenMO can create N virtual RF chains connected to N_{Ant} antennas, by utilizing N times oversampling ADC. However, using N virtual RF chains for handling N_{Ant} antennas does not allow for separate virtual RF chain per antenna as assumed in the previous sections. So a natural question is, how does GreenMO's techniques scale to larger number of antennas than number of virtual RF chains, and how does GreenMO still tap into the N_{ant} degrees of freedom with just N virtual RF chains?

The key advantage of GreenMO architecture which allows to effectively use N_{Ant} antennas' degrees of freedom is that virtual RF chains do not split up antenna array amongst themselves. Traditional beamformers which connect N_{Ant} antennas with N_{Ant} analog circuit elements, to N physical RF chains, end up dividing the N_{Ant} antenna array between the N RF chains. For example, say we have 8 antennas and 4 physical RF chains, we would get only 2 antennas per physical RF chain. However, virtual RF chains are just an abstraction over the single physically laid RF chain. In reality, all the 8 antennas here are simultaneously connected to the single physical RF chain, and thus the entire array is available to each of the virtual RF chain.

But how does GreenMO use these degrees of freedom to optimize for sampling+compute power? The insight here is to configure the antenna array differently for different virtual RF chain. The idea is that we can dedicate one virtual RF chain to just try and maximise the signal power for one user, and not worry about the interference suppression in the process. This is because the interference suppression can be taken care of via the digital precoding methods.

Put simply, we try and increase the signal power for user i in the i-th virtual RF chain. In order to do so, we would determine the maximal group of antennas in-phase for user i, and turn these antennas on for that virtual RF chain i. We name this algorithm to select the maximal in-phase antennas as BABF$(\cdot)$ (Algorithm 1), where BABF stands for Binarized Analog Beamforming. Essentially, for each virtual RF chain we try to beamform towards individual users using the $0-1$ bit control we have over the switched antenna array.

That is, with the BABF algorithm we get a switching matrix $\mathbf{B}$, where $\mathbf{B}$ is $N_{\text{Ant}} \times N$, which increases signal power of user i in the i-th virtual RF chain, by turning N_{Ant} antennas on-off strategically. In order to prioritize 1 user per virtual RF chain, BABF ends up projecting the $N \times N_{\text{Ant}}$ channel matrix $\mathbf{H}$, to an equivalent $N \times N$ channel matrix $\mathbf{HB}$. By prioritizing signal power for one user per virtual RF chain, we make $\mathbf{HB}$ as close to identity matrix as possible, by increasing the diagonal entries power (diagonal entries correspond to channel powers for user i for i-th virtual RF chain)

In summary, GreenMO's virtual architecture can also hybridize to support more number of antennas than virtual RF chains similar to the hybrid beamforming counterparts using analog circuits to connect more antennas to less number of physical RF chains. This allows GreenMO to effectively project the N_{ant} degrees of freedom to N streams, which optimizes for sampling+compute power, maintaining $O(n)$ power consumption rate for the sampling+compute power.

Thus, utilizing the virtual RF chains generated by GreenMO's design, a base station can ideally only consume the minimal of the power required in terms of RF front end ($O(1)$) and sampling+compute power ($O(N)$). Finally, GreenMO achieves this power optimization while maintaining the same signal spectrum of B and same data rates for the N users, by intuitive switching and NB sampling bandwidth. Additionally, this virtualization architecture of the RF-chains at the base stations provides them with the flexibility to handle increasing/decreasing user loads and always

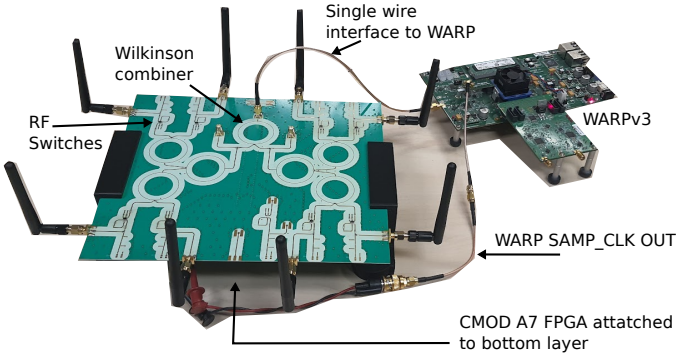

Figure 5: Hardware implementation of GreenMO

maintain the power consumption minimal. Thus achieving all the goals of a green communication architecture.

4 Implementation

We implement the GreenMO architecture on a custom multi-layer PCB prototype fabricated using Rogers substrate (as shown in Fig. 5). On the top-layer of the PCB, we design interfaces to utilize COTS antennas via SMA connectors, which are then connected to RF switches, and the output from 8 of these switched antennas is then combined with a wilkinson combiner network matched at the operating frequency for 2.4 GHz. On the bottom layer of the PCB, we have a CMOD-A7 FPGA used to clock the RF switches with appropriate switching sequences required to implement the switching matrix **B**. The FPGA is connected to a PC via a micro USB cable and allows us to program the RF switches to toggle in different configurations.

To implement this switching sequence correctly in hardware, we need to select RF switches with tON/tOFF below 25 ns, since otherwise the switches would be too slow to respond to the clocking input. For this we select the commercially avaialble switches HMC197BE[36] which have tRISE = 3 ns, and tON = 10 ns, suitable for our application. These switches have very minimal 0.5 dB insertion loss, and the overall insertion loss from the transmission lines in the PCB amount to about 3 dB. This is 10 dB lower than the current hybrid beamforming approach for sub-6 networks [27].

We utilize WARPv3 as the SDR for our implementation of an uplink receiver. The sampling clock for WARPv3 is 40 MHz, thus a sampling time period of 25 ns. Coming to the first design principle of GreenMO, which is to switch antennas on-off in order to create the time interleaved virtual RF chains, we need to switch the antennas on-off in a way that this switching is synchronised with the sampling instants of the SDR. WARPv3 exposes it's sampling clock using the CM-MMCX module, which is then fed to the FPGA, and the FPGA utilizes this sampling clock to then derive the switching frequencies.

Since we create $K = 4$ virtual RF chains by our switching, in order to support $K = 4$ users, we fix the bandwidth of transmitters to be 10 MHz. These 10 MHz transmitters are implemented on different SBX daughterboards on USRP. Note that this choice of transmit bandwidth is constraint because of our choice of receiver SDR, as with WARPv3 we can not do more than 40 MHz sampling (since the MAX2829 IC used in WARP has a maximum RF bandwidth of 40 MHz). The transmitting USRPs and the receiving WARP are not synchronized and share a different clock altogether. We have observed that the CFO introduced as a consequence of unsynch TX-RX doesnt play any role in GreenMO's performance, as essentially GreenMO utilizes a spatial operation, and because of CFO we have some constant phase offsets across the virtual RF chains which are naturally compensated during channel estimation.

Finally, to implement the required digital signal processing, we utilize the WARPLab codes in MATLAB to utilize 802.11 compliant OFDM waveform with 64 subcarriers (48 data, 4 pilots and 12 null subcarriers), with the required tweaks to create and utilize these time interleaved RF chains. The channel estimation is done by having the users transmit LTS's separately from each other, and after the last user's LTS is finished the common data transmission mode starts. Using the estimated channels from the LTS preamble, we calculate the best switching matrix,**B** based on BABF algorithm, and configure the CMOD FPGA via UART communication to implement the switching sequences corresponding to **B** and then collect the received samples having the equivalent channel of **HB**.

For the experiments we set the transmit power such that we have SNR of about 17-20 dB, and utilize QAM-16 constellation with 0.5 rate convolutional channel code. This choice of SNRs is consistent with the recent works on MIMO systems [8]. This constellation was tested to work reliably for these SNRs, given the phase noise of our implementation with users on an USRP and AP being WARPv3.

5 Evaluations

GreenMO creates the first multi-antenna architecture which has the capability of handling multi-user transmissions while optimizing both the RF front end power consumption, as well as sampling+compute power efficiency. In this section, we evaluate GreenMO to justify each of these claims.

5.1 Evaluation Setting:

We evaluate the power consumption, SINR, system capacity, Goodput and Energy per joule performance for 2,3,4 users at various positions in a conference room setting (Fig. 6a), to capture the overall performance trends in the experimental setting considered. The room which we choose has rough dimensions of 12m*5m, and is populated with objects like

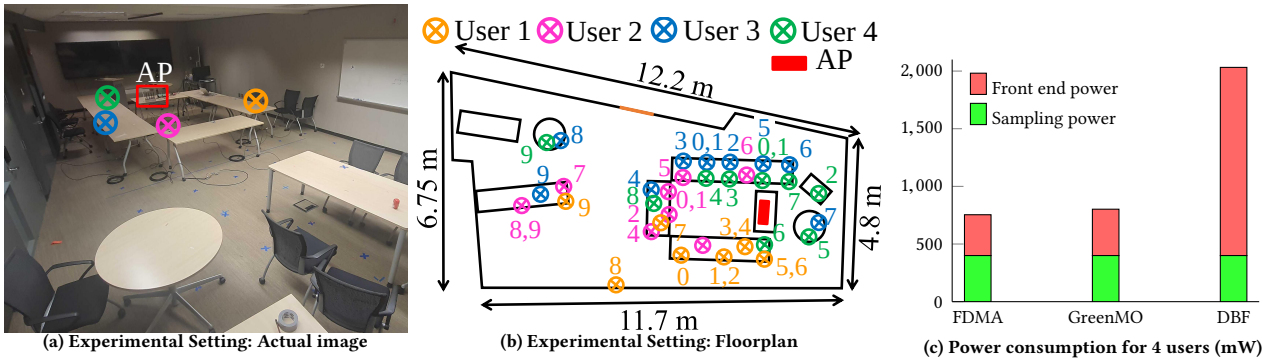

(a) Experimental Setting: Actual image (b) Experimental Setting: Floorplan (c) Power consumption for 4 users (mW)

Figure 6: We test GreenMO in a conference room setting (a), and the numbers 0, 1, . . . 9 in (b) represent the 4 user positions for the 10 configurations where we test GreenMO and baselines, (c) shows the power consumption metrics of our setup

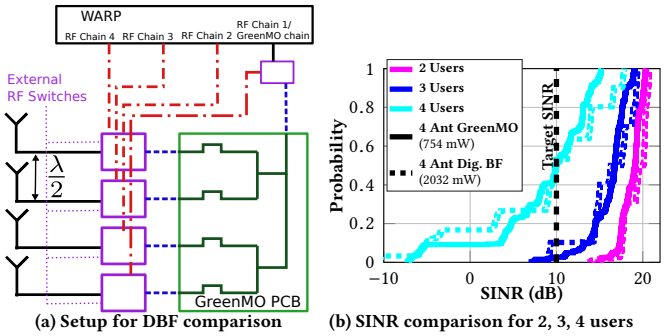

(a) Setup for DBF comparison (b) SINR comparison for 2, 3, 4 users

Figure 7: Baseline comparisons with DBF

tables, chairs, whiteboard and TV screens, which make the setting rich with scattering effects. We implement 5 different test configurations and baselines: 4 antenna GreenMO, 4 antenna DBF, 8 antenna GreenMO, 8 antenna DBF (Trace level) and Interference free FDMA oracle.

5.2 RFE and Sampling power consumption: WARPv3's RF transceiver MAX2829 [37], performs the downconversion and filtering. From the datasheet, we can see that 4 antenna DBF would require RFE power of 1632 mW (4×408 mW) power when operating in synchronous MIMO mode, while only 354 mW for GreenMO operating by itself, as is the case with GreenMO and interference-free oracle which employs FDMA. Finally, GreenMO uses a network of switches for creating per-antenna spectrum variations leading to virtual RF chain creation; This has near negligible power consumption, similar to how these switches being used for backscatter communications which exploit this near negligible power for battery-less operation. The HMC197BE switches used in GreenMO design require just 0.001 mW of static power, and even including the active power they draw from the MHz clock sources, it is fairly less than 1 mW. Hence total RFE power consumption for 8 antenna GreenMO is approximately 354+8 = 362 mW (assuming 1mW per switch), for FDMA it is 354 mW and for DBF it is 1632 mW.

ADC power varies linearly with the sampling frequency [17], which is true for the AD9963 ADC used for WARP, as evident from the datasheet [38]. Thus, the power consumption of 4 ADCs is same to that of one ADC with 4x higher sampling. From the datasheets of AD9963, we have power consumption as 400 mW for 40 MHz sampling operation used for GreenMO and FDMA, whereas 4 physical RF chains with 10 MHz would use 4*100 = 400 mW as well. Thus for all the three confiurations, the sampling power would be 400mW.

Therefore, total power consumption of GreenMO is 762 mW (354+400+8 mW) which is 3x lower than MIMO (1632+400 = 2032 MW), and almost the same as single antenna FDMA oracle, which would be 754 mW (354+400mW).

Fig. 6c shows the power consumption metrics for each of the strategy. As seen clearly, it is not the sampling power which dominates the power consumption, but the power consumed in the front end by these multiple RF chains.

5.3 SINR performance comparison of 4 antenna GreenMO with DBF: GreenMO is the first work to use virtual RF chains. Hence, it is important to show the performance comparison with physical RF chains. We do so by creating a faithful test setup to compare virtual RF chains with physical RF chains (Fig. 7a). Basically we use external switches to have the same antennas connected to either 4 physical RF chains directly, or 4 virtual RF chains via RF switched array. Thus, we can compare the 2 approaches faithfully, as both of them capture the samples from the same antennas.

The SINR performance of both the methods indeed turn out to be very similar (Fig. 7b). For these CDFs, we collect 30 packets at each of the 10 locations of 4 users in the conference room, which gives 300 sample SINRs these plots. We can clearly see the performance for both the methods to be very similar (within ± 0.5 dB for median error). Thus 4 virtual RF chains, with total power consumption as 762 mW provides same SINR metrics as 4 physical RF chains, with total power consumption 2032 mW, which is 3x more than GreenMO. However, as the number of users increase from 2 to 4, the performance of both the two approaches

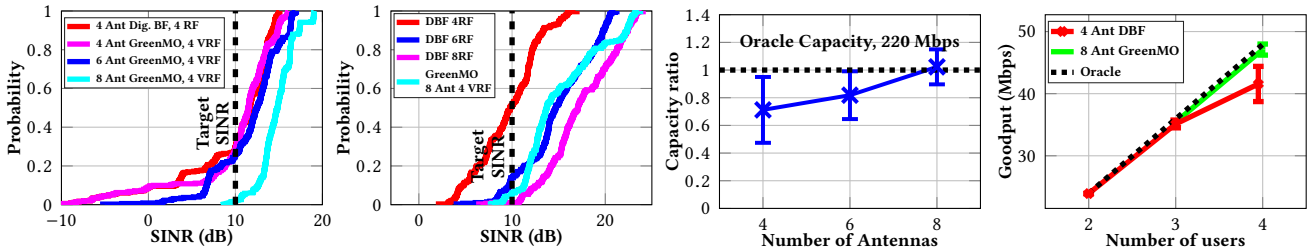

(a) 8 Ant GreenMO improves SINR for 4 users (b) Trace level comparisons with 8 antenna DBF (c) Increasing number of antennas allow reaching FDMA capacity (d) Throughput results

Figure 8: Experiment CDFs for SINR plotted across multiple packets collected for multiple user locations in the conference room setting, and Average Goodput with errorbars representing std. deviation across multiple packets. We can see that with 8×4 GreenMO, we always meet the target SINR which allows robust goodput performance for all users, and also meets FDMA oracle capacity

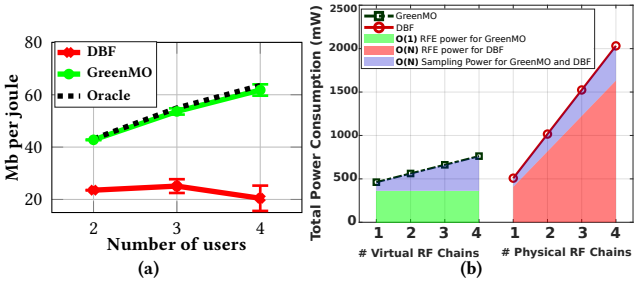

Figure 9: (a) Energy Efficiency and (b) Power consumption with number of RF Chains

deteriorate, and with 4 users, for almost 40% of the packets, the SINR is lesser than 10 dB (Fig. 7b).

5.4 Optimizing sampling+compute power by serving 4 users reliably with 4 virtual RF chains: In order to improve the performance as number of users N approach number of virtual RF chains N, we increase the antennas and use our BABF algorithm to prioritize 1 user per RF chain.

For this experiment, we use the GreenMO PCB which has the capability to utilize 8 switched antennas, and create 4 virtual RF chains from the combined 8 antenna output. We can electronically turn off antennas in our PCB to simultaneously collect data from 4, as well as 6 antenna configurations to understand the effect of increasing number of antennas on the system metrics. The SINR and goodput results are shown in Fig. 8a. As we increase the antennas to 8, the SINR shows an immense jump and always exceeds 10 dB, close to what is expected from a robust multi-user transmission scheme. We observe more than 10 dB increase in the 90-th percentile SINR, as compared to 4 antenna digital beamformer implemented using WARP's physical RF chains.

Unlike GreenMO, digital beamforming approaches utilize a naive way of improving performance for 4 users, which is to add more RF chains to sample from more antennas. Since WARPv3 has support only for 4 physical RF chains, we do a trace level comparison to 6, 8 RF chain DBF by collecting 4 antennas channels at a time and then synchronizing them in post-processing. We observe that GreenMO even outperforms a 6 antenna digital beamformer (Fig. 8b), and comes $\sim$ 3 dB close to 8 antenna digital beamformer at median performachainsnce, all the while having at least 4x lower power consumption.

5.5 Comparison with interference-free oracle: For the FDMA oracle, the users occupy 4 different 10 MHz bands, and the WARP would sample this aggregate 40 MHz bandwidth in order to serve these 4 non-interfering users. In contrast, for GreenMO, the 4 users occupy the same 10 MHz band, and the WARP receiver samples a higher sampling bandwidth 40 MHz, in order to create the 4 virtual RF chains required to multiplex the 4 users signals. Thus in order to be spectrum-efficient, GreenMO has to cancel the in-band interference in the occupied 10 MHz bandwidth Even with added task of interference cancellation, we see that with more number of antennas (8) than number of users (4), we get system capacity on on par with FDMA oracle (Fig. 8c).

5.6 Energy efficiency metrics (bits per joules): Finally, we revisit the power calculations briefly in the context of our goodput results. As seen in Fig. 8d, we can get goodput close to interference-free oracle levels using GreenMO architecture with 8 antennas. This result can also be viewed in the lens of bits per joules (Fig. 9a) by seeing how much power got expended in the process. As the number of RF chains increase from 2 to 4, we see constant $O(1)$ 354 mW RF front end (RFE) power demand for GreenMO, as explained in Section 5.2. The ADC power requirements are $100mW$ per 10 MHz data sampled and that increases as $O(N)$ with users. On the other end, for digital beamforming, RFE power scales linearly with N, given by $408 * N$, since the WARPv3 MAX2829 IC uses 408 mW per RF chain in MIMO mode. Hence, we get energy consumption trends as shown in Fig. 9b. This explains the energy per joule Fig. 9a, more particularly, the dip for DBF at 4 user operation. This is because, the DBF goodput shows a downward trend for 4 users, whereas power has kept on increasing linearly, which further exacerbates the energy efficiency between DBF and GreenMO.

5.7 Ablation studies:

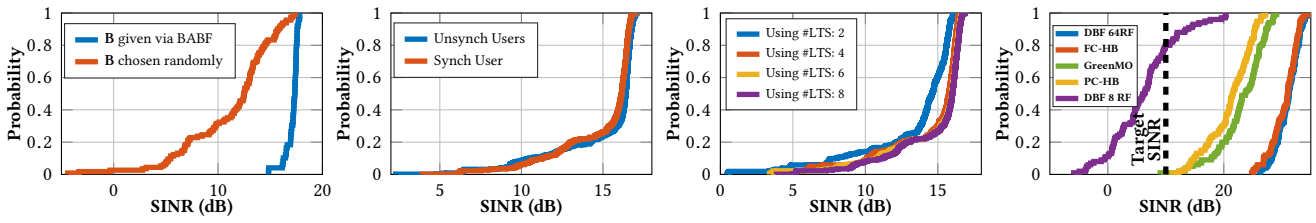

(a) Choice of S (b) Synch. vs Unsynch. users (c) Varying channel estimation accuracy (d) Large scale simulations

Figure 10: Ablation studies to adjudge GreenMO's performance (a)-(c), and a large scale simulation result (d)

First, to evaluate the effectiveness of BABF, we choose 100 random choices of **B**, and collect 10 packets with each choice, and repeat the same with 100 packets collected by choosing **B** via BABF algorithm which chooses in-phase switches for one user per virtual RF chain. We plot the CDF in Fig. 10a, and observe that BABF **B** matrix always outperforms a randomly chosen **B**.

Second, to show robustness against unsynchronized users, we first synchronize the users to each other by utilizing same reference clock and start time, and thus all the transmitters have same CFO and tightly synchronized sampling times. Then, we repeat the experiment by having unsynchronized usees, suchthat each user has a different clock, leading to different CFOs for each user. As clearly seen from Fig. 10b, we get almost the same performance when the transmitters are synchronised with each other as compared to when they are unsynchronized.

Third, the interference cancellation performance also depends on the accuracy of channel estimates procured. We can always average the channel across multiple LTS's to get a higher channel estimation accuracy. Thus, we repeat the experiment with more number of LTS's than the prescribed 2 LTS's as per 802.11 protocol, and observe that we get only about 1.5 dB difference in median performance as the number of LTS's increase to 10, which shows that GreenMO's algorithms can work without imposing a high cost of channel estimation latency.

6 Discussion and Future Work

Scaling to higher number of antennas and users: Although our hardware experiments are limited to handling 4 users, partly because of our evaluation platform WARPv3 which supports only 40 MHz sampling and also partly because the RF switch we use has about $\sim 3ns$ rise time and $\sim 10ns$ on time, so we can not handle faster bandwidth switching than 50 MHz. However, the techniques introduced in this paper are fairly general and can be implemented for higher number of antennas and more number of users.

To motivate this, we perform simulations by placing users in similar environments to our evaluation setting, and model the wireless channel via ray-tracing. The users transmit similar OFDM signals to our evaluation setting as well, and the channels are applied to the OFDM waveform by calculating the distances from the environment scaterrors and applying appropriate time delays+amplitude weights in the received OFDM signal. All the receieve processing uses the identical codes used for hardware evaluations. Hence, this simulation framework gives results which by and large follow the trends expected from experimental evaluations.

Fig. 10d shows simulation results and comparison for 64 antennas usecase to serve 8 users. This is considered a standard baseline with multi-user Dense deployments, which on an average require serving 8 streams concurrently [9]. GreenMO uses 64 antennas and creates 8 virtual RF chains to serve the 8 users, and almost always obtains >10dB SINR. We can see even in simulations serving 8 users with 8 RF chain digital beamforming is infeasible. We also show comparisons with ideal partially and fully connected hybrid beamformers with 8 physical RF chains. Our simulations assume perfect phase quantization, and still GreenMO outperforms partially connected beamformers. The reason is that unlike partially connected beamformers GreenMO does not split the antenna array between the physical RF chains, since all the antennas are by default connected to the virtual RF chains.

GreenMO's performance comes about $5dB$ close on an average, to the full 64 chain DBF and fully connected HB, even though using at least 64x lower power and 64x lower circuit elements.

Scaling to wider bandwidths: In this paper, we have evaluated GreenMO for a maximum of 4 users having a bandwidth of 10 MHz. However, GreenMO architecture can easily scale to wider-bandwidth. The two key component of GreenMO architecture are switches and ADCs. There are easily available ADCs now capable of 1 GHz sampling bandwidth [39, 40], which can easily support 50 virtual chain at 20 MHz sampling, typical bandwidth for most sub-6 GHz communication. The improvement in ADC technology is to enable mmWave frequencies, which is rarely deployed. Today, more than 95% devices operate in sub-6 band [41], and GreenMO architecture gives an application where these ADCs can be developed to serve more users in sub-6 and alleviate the spectrum crunch we have today with sub-6 devices.

Next, the needs for fast switches, as GreenMO has these switches at the heart of the architecture. Photonic RF

switches under development in research labs offer picosecond rise time[42–44], alongwith a few commercially available switches offering sub-ns rise times[45], easily can enable 1 GHz switching speed. GreenMO's architecture can lead to these switches being common in the circuits marketplace. Thus, integration with high sample rate ADCs and picosecond fast RF switches would form a future direction for GreenMO architecture

Augmenting GreenMO with RF filters: Due to the frequency shifts created by the RF switches, if there are coexisting neighbouring band transmissions, these will also get frequency shifted and fall into the spectrum band of interest. Thus, in addition to RF switches, GreenMO design also required RF filters which would clean up the sampled spectrum before the switching. There are WiFi channel filters [46, 47] available which can satisfy the requirements posed by GreenMO architecture to clean up the sampled spectrum, and we will be augmenting our PCB prototype with these filters as an imemdiate next step.

7 Related Works

GreenMO presents a spectrum efficient, power-efficient and flexible multi-user communication architecture using a single physical RF chain. We have already discussed comparisons of GreenMO with Hybrid and Digital beamformers in Section 2. In this section we will compare to new upcoming architectures and past theory work.

Hence, previously proposed MIMO interfaces which utilize just a single RF chain [48–50] form the closest of past work related to GreenMO. These set of works also utilize a higher IF bandwidth than the users' transmitted bandwidth. However, instead of combining over time and enabling creation of virtual digital RF chains, these works implement analog beamforming and utilize the higher bandwidth only to multiplex the outputs from these analog beamforming blocks. Put more simply, these works either use IF bandwidth code domain [48, 49] or different freq. bands in the higher IF bandwidth [50] to multiplex the outputs from a prior analog beamforming front-end. The challenge with these works is that the analog beamforming component also needs to do beam-nulling, which is not very robust to wideband operation and phase shifter inaccuracies [51]. In contrast, for GreenMO architecture, the final interference cancellation block in GreenMO is fully digital and hence GreenMO can do wideband digital combining, as well as phase combining with arbitrary accuracy, which makes it stand out of the prior art on single-wire MIMO interfaces.

There are also a parallel set of works which explore parasitic antenna arrays to create artificial temporal changes in the channel [52–59], as well as a body of works on Time Modulated Antenna Arrays (TMAA) [60–71]. Both these body of works propose something on the lines of GreenMO; The first body of works switching impedences of the parasitic antenna array, and the second set of works modulate the antenna array with fast toggling RF switches. Both of them are similar to how GreenMO creates the frequency shifts using the RF switches. However, most of the prior effort is leveraging time-diversity to improve the diversity gains or throughput of single user instead of facilitating multi-user. Also, the experimental evaluations have not considered OFDM, or even higher constellation like QAM16 on narrowband systems with these methods. For switching impedances of the parasitic array, there are known issues on the technique not scaling well with number of antennas [58], and requires precision control over antenna impedance to generate the required orthogonal beams [57]. The most notable of the TMAA set of works utilize a 4 antenna array and a 50 MHz switching speed to allow for increased diversity gains while decoding with a single RF chain [61–63, 65, 71]. However, this has only be demonstrations are again limited to single user. Even for single user, there is no practical implementation extending these ideas to OFDM. and thus to the best of our knowledge, GreenMO remains the first practical demonstration of a RF switch based antenna array utilizing high switching rate and OFDM transmissions supporting multi-users and higher order constellations like QAM-16.

Some papers have proposed to extend antenna arrays by means of stitching sub-arrays together via RF switches; mainly to improve spatial localization accuracy or bring in additional antenna selection gains to communications [72, 73]. However, these works use static switches, whereas in GreenMO switches are actively switching at baseband frequencies and the effect created by this fast switching is very different. There are other papers which target the uplink MIMO problem as well, with some of them requiring coordination from the users to do interference alignment [74, 75], set random delays in transmissions to break channel correlations [76], or utilize distributed APs to serve multiple users [77]. Also, there are papers on selecting group of users which can be served efficiently with standard mu-MIMO architectures employing $M = K$, which require a strategic scheduler to manage the multi-user network [78–80]. However, in contrast, GreenMO utilizes just a single AP and demands no special coordination from the clients, and hence the clients by default are COTS compliant. Further, we make the multiplexing gains robust for any set of user groupings, by utilizing $M > K$ antennas however still utilizing similar sampling costs.

References

[1] The wireless communications industry and its carbon footprint. https://www.azocleantech.com/article.aspx?ArticleID=1131.

[2] How to estimate carbon emissions in mobile networks: a streamlined approach. https://www.ericsson.com/en/blog/2021/5/how-to-estimate-carbon-emissions-from-mobile-networks.

[3] S Sinha. State of iot 2021: Number of connected iot devices growing 9% to 12.3 billion globally, cellular iot now surpassing 2 billion. *IoT Analytics: Market Insights for the Internet of Things*, 2021.

[4] Teena Sharma, Abdellah Chehri, and Paul Fortier. Review of optical and wireless backhaul networks and emerging trends of next generation 5g and 6g technologies. *Transactions on Emerging Telecommunications Technologies*, 32(3):e4155, 2021.

[5] U.s. airline group warns 5g interference issues could linger for years. https://www.reuters.com/business/aerospace-defense/us-airline-group-warns-5g-interference-issues-could-linger-years-2022-02-01/.

[6] How the faa went to war against 5g. https://www.cnet.com/tech/mobile/how-the-faa-went-to-war-against-5g/.

[7] Wi-fi 6:the next generation of wireless. https://meraki.cisco.com/lib/pdf/meraki_whitepaper_wifi6.pdf.

[8] Jian Ding, Rahman Doost-Mohammady, Anuj Kalia, and Lin Zhong. Agora: Real-time massive mimo baseband processing in software. In *Proceedings of the 16th International Conference on emerging Networking EXperiments and Technologies*, pages 232–244, 2020.

[9] Han Yan, Sridhar Ramesh, Timothy Gallagher, Curtis Ling, and Danijela Cabric. Performance, power, and area design trade-offs in millimeter-wave transmitter beamforming architectures. *IEEE Circuits and Systems Magazine*, 19(2):33–58, 2019.

[10] Daniel C Araújo, Taras Maksymyuk, André LF de Almeida, Tarcisio Maciel, João CM Mota, and Minho Jo. Massive mimo: survey and future research topics. *Iet Communications*, 10(15):1938–1946, 2016.

[11] Jakob Hoydis, Stephan Ten Brink, and Mérouane Debbah. Massive mimo in the ul/dl of cellular networks: How many antennas do we need? *IEEE Journal on selected Areas in Communications*, 31(2):160–171, 2013.

[12] Lingjia Liu, Runhua Chen, Stefan Geirhofer, Krishna Sayana, Zhihua Shi, and Yongxing Zhou. Downlink mimo in lte-advanced: Su-mimo vs. mu-mimo. *IEEE Communications Magazine*, 50(2):140–147, 2012.

[13] Eduardo Castaneda, Adao Silva, Atilio Gameiro, and Marios Kountouris. An overview on resource allocation techniques for multi-user mimo systems. *IEEE Communications Surveys & Tutorials*, 19(1):239–284, 2016.

[14] Susnata Mondal, Rahul Singh, Ahmed I Hussein, and Jeyanandh Paramesh. A 25–30 GHz fully-connected hybrid beamforming receiver for MIMO communication. *IEEE Journal of Solid-State Circuits*, 53(5):1275–1287, 2018.

[15] Susnata Mondal, Rahul Singh, Ahmed I Hussein, and Jeyanandh Paramesh. A 25-30 GHz 8-antenna 2-stream hybrid beamforming receiver for MIMO communication. In *2017 IEEE Radio Frequency Integrated Circuits Symposium (RFIC)*, pages 112–115. IEEE, 2017.

[16] Susnata Mondal, Rahul Singh, and Jeyanandh Paramesh. 21.3 a reconfigurable bidirectional 28/37/39GHz front-end supporting MIMO-TDD, carrier aggregation TDD and FDD/Full-duplex with self-interference cancellation in digital and fully connected hybrid beamformers. In *2019 IEEE International Solid-State Circuits Conference-(ISSCC)*, pages 348–350. IEEE, 2019.

[17] C Nicolas Barati, Sourjya Dutta, Sundeep Rangan, and Ashutosh Sabharwal. Energy and latency of beamforming architectures for initial access in mmwave wireless networks. *Journal of the Indian Institute of Science*, 100(2):281–302, 2020.

[18] Pengyu Zhang, Dinesh Bharadia, Kiran Joshi, and Sachin Katti. Hitchhike: Practical backscatter using commodity wifi. In *Proceedings of the 14th ACM Conference on Embedded Network Sensor Systems CD-ROM*, pages 259–271, 2016.

[19] Pengyu Zhang, Colleen Josephson, Dinesh Bharadia, and Sachin Katti. Freerider: Backscatter communication using commodity radios. In *Proceedings of the 13th International Conference on emerging Networking EXperiments and Technologies*, pages 389–401, 2017.

[20] Manideep Dunna, Miao Meng, Po-Han Wang, Chi Zhang, Patrick P Mercier, and Dinesh Bharadia. Syncscatter: Enabling wifi like synchronization and range for wifi backscatter communication. In *NSDI*, pages 923–937, 2021.

[21] Xin Liu, Zicheng Chi, Wei Wang, Yao Yao, and Ting Zhu. Vmscatter: A versatile {MIMO} backscatter. In *17th {USENIX} Symposium on Networked Systems Design and Implementation ({NSDI} 20)*, pages 895–909, 2020.

[22] Bryce Kellogg, Aaron Parks, Shyamnath Gollakota, Joshua R Smith, and David Wetherall. Wi-fi backscatter: Internet connectivity for rf-powered devices. In *Proceedings of the 2014 ACM Conference on SIGCOMM*, pages 607–618, 2014.

[23] A Lee Swindlehurst, Ender Ayanoglu, Payam Heydari, and Filippo Capolino. Millimeter-wave massive mimo: The next wireless revolution? *IEEE Communications Magazine*, 52(9):56–62, 2014.

[24] MinKeun Chung, Liang Liu, Andreas Johansson, Martin Nilsson, Olof Zander, Zhinong Ying, Fredrik Tufvesson, and Ove Edfors. Millimeter-wave massive mimo testbed with hybrid beamforming. In *2020 54th Asilomar Conference on Signals, Systems, and Computers*, pages 309–313. IEEE, 2020.

[25] Greg LaCaille, Antonio Puglielli, Elad Alon, Borivoje Nikolic, and Ali Niknejad. Optimizing the lo distribution architecture of mm-wave massive mimo receivers. *arXiv preprint arXiv:1911.01339*, 2019.

[26] Hong-Teuk Kim, Byoung-Sun Park, Seong-Sik Song, Tak-Su Moon, So-Hyeong Kim, Jong-Moon Kim, Ji-Young Chang, and Yo-Chul Ho. A 28-GHz cmos direct conversion transceiver with packaged 2*4 antenna array for 5G cellular system. *IEEE Journal of Solid-State Circuits*, 53(5):1245–1259, 2018.

[27] Thomas Kühne, Piotr Gawłowicz, Anatolij Zubow, Falko Dressler, and Giuseppe Caire. Bringing hybrid analog-digital beamforming to commercial MU-MIMO wifi networks. In *Proceedings of the 26th Annual International Conference on Mobile Computing and Networking*, pages 1–3, 2020.

[28] Yasaman Ghasempour, Muhammad K Haider, Carlos Cordeiro, Dimitrios Koutsonikolas, and Edward Knightly. Multi-stream beam-training for mmWave MIMO networks. In *Proceedings of the 24th Annual International Conference on Mobile Computing and Networking*, pages 225–239, 2018.

[29] Xiufeng Xie, Eugene Chai, Xinyu Zhang, Karthikeyan Sundaresan, Amir Khojastepour, and Sampath Rangarajan. Hekaton: Efficient and practical large-scale MIMO. In *Proceedings of the 21st Annual International Conference on Mobile Computing and Networking*, pages 304–316, 2015.

[30] Yongce Chen, Yan Huang, Chengzhang Li, Y Thomas Hou, and Wenjing Lou. Turbo-HB: A novel design and implementation to achieve ultra-fast hybrid beamforming. In *IEEE INFOCOM 2020-IEEE Conference on Computer Communications*, pages 1489–1498. IEEE, 2020.

[31] Didi Zhang, Yafeng Wang, Xuehua Li, and Wei Xiang. Hybridly connected structure for hybrid beamforming in mmWave massive MIMO systems. *IEEE Transactions on Communications*, 66(2):662–674, 2017.

[32] Xianghao Yu, Juei-Chin Shen, Jun Zhang, and Khaled B Letaief. Alternating minimization algorithms for hybrid precoding in millimeter wave MIMO systems. *IEEE Journal of Selected Topics in Signal Processing*, 10(3):485–500, 2016.

[33] Tatsunori Obara, Tatsuki Okuyama, Yuuichi Aoki, Satoshi Suyama, Jaekon Lee, and Yukihiko Okumura. Indoor and outdoor experimental trials in 28-GHz band for 5G wireless communication systems. In *2015 IEEE 26th Annual International Symposium on Personal, Indoor, and Mobile Radio Communications (PIMRC)*, pages 846–850. IEEE, 2015.

[34] Zhe Chen, Xu Zhang, Sulei Wang, Yuedong Xu, Jie Xiong, and Xin Wang. BUSH: empowering large-scale MU-MIMO in WLANs with hybrid beamforming. In *IEEE INFOCOM 2017-IEEE Conference on*

Computer Communications, pages 1–9. IEEE, 2017.

[35] Manideep Dunna, Chi Zhang, Daniel Sievenpiper, and Dinesh Bharadia. Scattermimo: Enabling virtual mimo with smart surfaces. In *Proceedings of the 26th Annual International Conference on Mobile Computing and Networking*, pages 1–14, 2020.

[36] HMC197BE. https://www.analog.com/media/en/technical-documentation/data-sheets/hmc197b.pdf.

[37] MAX2829. https://datasheets.maximintegrated.com/en/ds/MAX2828-MAX2829.pdf.

[38] AD9963. https://www.analog.com/en/products/ad9963.html.

[39] ADC captures 1Gsps. https://www.maximintegrated.com/en/design/technical-documents/app-notes/6/642.html.

[40] 1 GHz ADC from TI. https://www.ti.com/lit/ug/tidubq0/tidubq0.pdf.

[41] Number of 4g lte connections worldwide from 2012 to 2020. https://www.statista.com/statistics/736022/4g-lte-connections-worldwide/.

[42] Jia Ge and Mable P Fok. Ultra high-speed radio frequency switch based on photonics. *Scientific reports*, 5(1):1–7, 2015.

[43] Yiwei Xie, Leimeng Zhuang, Pengcheng Jiao, and Daoxin Dai. Sub-nanosecond-speed frequency-reconfigurable photonic radio frequency switch using a silicon modulator. *Photonics Research*, 8(6):852–857, 2020.

[44] Hengyun Jiang, Lianshan Yan, Wei Pan, Bing Luo, and Xihua Zou. Ultra-high speed RF filtering switch based on stimulated brillouin scattering. *Optics letters*, 43(2):279–282, 2018.

[45] Hmmc2027 gaas rf switch. https://www.acalbfi.com/be/RF-components/Switches/p/DC---26-5-{GHz}-SPDT-Absorptive-GaAs-Switch-IC/0000000JUM.

[46] Saw filter qpq1906. https://www.crystek.com/microwave/spec-sheets/filter/CBPFS-2441.pdf.

[47] Qorvo qpq1906. https://www.mouser.com/datasheet/2/412/QPQ1906_Data_Sheet-1795086.pdf.

[48] Fred Tzeng, Amin Jahanian, Deyi Pi, and Payam Heydari. A cmos code-modulated path-sharing multi-antenna receiver front-end. *IEEE journal of solid-state circuits*, 44(5):1321–1335, 2009.

[49] Manoj Johnson, Armagan Dascurcu, Kai Zhan, Arman Galioglu, Naresh Kumar Adepu, Sanket Jain, Harish Krishnaswamy, and Arun S Natarajan. Code-domain multiplexing for shared IF/LO interfaces in millimeter-wave MIMO arrays. *IEEE Journal of Solid-State Circuits*, 55(5):1270–1281, 2020.

[50] Robin Garg, Gaurav Sharma, Ali Binaie, Sanket Jain, Sohail Ahasan, Armagan Dascurcu, Harish Krishnaswamy, and Arun S Natarajan. A 28-GHz beam-space MIMO RX with spatial filtering and frequency-division multiplexing-based single-wire IF interface. *IEEE Journal of Solid-State Circuits*, 2020.

[51] Sohrab Madani, Suraj Jog, Jesús Omar Lacruz, Joerg Widmer, and Haitham Hassanieh. Practical null steering in millimeter wave networks. In *NSDI*, pages 903–921, 2021.

[52] Osama N Alrabadi, Chamath Divarathne, Philippos Tragas, Antonis Kalis, Nicola Marchetti, Constantinos B Papadias, and Ramjee Prasad. Spatial multiplexing with a single radio: Proof-of-concept experiments in an indoor environment with a 2.6-GHz prototype. *IEEE Communications Letters*, 15(2):178–180, 2010.

[53] Bo Han, Vlasis I Barousis, Constantinos B Papadias, Antonis Kalis, and Ramjee Prasad. MIMO over ESPAR with 16-QAM modulation. *IEEE Wireless Communications Letters*, 2(6):687–690, 2013.

[54] Heung-Gyoon Ryu and Bong-Jun Kim. Beam space MIMO-OFDM system based on ESPAR antenna. In *2015 International Workshop on Antenna Technology (iWAT)*, pages 168–171. IEEE, 2015.

[55] Yafei Hou, Rian Ferdian, Satoshi Denno, and Minoru Okada. Low-complexity implementation of channel estimation for ESPAR-OFDM receiver. *IEEE Transactions on Broadcasting*, 67(1):238–252, 2020.

[56] Illsoo Sohn and Donghyuk Gwak. Single-RF MIMO-OFDM system with beam switching antenna. *EURASIP Journal on Wireless Communications and Networking*, 2016(1):1–14, 2016.

[57] Junho Lee, Ju Yong Lee, and Yong H Lee. Spatial multiplexing of OFDM signals with QPSK modulation over ESPAR. *IEEE Transactions on Vehicular Technology*, 66(6):4914–4923, 2016.

[58] Zixiang Han, Yujie Zhang, Shanpu Shen, Yue Li, Chi-Yuk Chiu, and Ross Murch. Characteristic mode analysis of ESPAR for single-RF MIMO systems. *IEEE Transactions on Wireless Communications*, 20(4):2353–2367, 2020.

[59] Jung-Nam Lee, Yong-Ho Lee, Kwang-Chun Lee, and Tae Joong Kim. $\lambda/64$-spaced compact ESPAR antenna via analog RF switches for a single RF chain MIMO system. *ETRI Journal*, 41(4):536–548, 2019.

[60] Gweondo Jo, Hyoung-Oh Bae, Donghyuk Gwak, and Jung-Hoon Oh. Demodulation of 4× 4 MIMO signal using single RF. In *2016 18th International Conference on Advanced Communication Technology (ICACT)*, pages 390–393. IEEE, 2016.

[61] Grzegorz Bogdan, Konrad Godziszewski, and Yevhen Yashchyshyn. MIMO receiver with reduced number of RF chains based on 4D array and software defined radio. In *2019 27th European Signal Processing Conference (EUSIPCO)*, pages 1–5. IEEE, 2019.

[62] Grzegorz Bogdan, Konrad Godziszewski, Yevhen Yashchyshyn, Cheol Ho Kim, and Seok-Bong Hyun. Time-modulated antenna array for real-time adaptation in wideband wireless systems–part i: Design and characterization. *IEEE Transactions on Antennas and Propagation*, 68(10):6964–6972, 2019.

[63] Grzegorz Bogdan, Konrad Godziszewski, and Yevhen Yashchyshyn. Time-modulated antenna array for real-time adaptation in wideband wireless systems–part ii: Adaptation study. *IEEE Transactions on Antennas and Propagation*, 68(10):6973–6981, 2020.

[64] José P González-Coma and Luis Castedo. Wideband hybrid precoding using time modulated arrays. *IEEE Access*, 8:144638–144653, 2020.

[65] Grzegorz Bogdan, Konrad Godziszewski, and Yevhen Yashchyshyn. Time-modulated antenna array with beam-steering for low-power wide-area network receivers. *IEEE Antennas and Wireless Propagation Letters*, 19(11):1876–1880, 2020.

[66] Wen-Qin Wang, Hing Cheung So, and Alfonso Farina. An overview on time/frequency modulated array processing. *IEEE Journal of Selected Topics in Signal Processing*, 11(2):228–246, 2016.

[67] José P González-Coma, Roberto Maneiro-Catoira, and Luis Castedo. Hybrid precoding with time-modulated arrays for mmwave MIMO systems. *IEEE Access*, 6:59422–59437, 2018.

[68] Avishek Chakraborty, Gopi Ram, and Durbadal Mandal. Time-modulated multibeam steered antenna array synthesis with optimally designed switching sequence. *International Journal of Communication Systems*, 34(9):e4828, 2021.

[69] Chong He, Xianling Liang, Bin Zhou, Junping Geng, and Ronghong Jin. Space-division multiple access based on time-modulated array. *IEEE Antennas and Wireless Propagation Letters*, 14:610–613, 2014.

[70] Roberto Maneiro-Catoira, Julio Brégains, José A García-Naya, and Luis Castedo. Time modulated arrays: From their origin to their utilization in wireless communication systems. *Sensors*, 17(3):590, 2017.

[71] Grzegorz Bogdan, Miłosz Jarzynka, and Yevhen Yashchyshyn. Experimental study of signal reception by means of time-modulated antenna array. In *2016 21st International Conference on Microwave, Radar and Wireless Communications (MIKON)*, pages 1–4. IEEE, 2016.

[72] Yaxiong Xie, Yanbo Zhang, Jansen Christian Liando, and Mo Li. Swan: Stitched wi-fi antennas. In *Proceedings of the 24th Annual International Conference on Mobile Computing and Networking*, pages 51–66, 2018.

[73] Zhihao Gu, Taiwei He, Junwei Yin, Yuedong Xu, and Jun Wu. Tyrloc: a low-cost multi-technology mimo localization system with a single rf chain. In *Proceedings of the 19th Annual International Conference on*

Mobile Systems, Applications, and Services, pages 228–240, 2021.

[74] Shyamnath Gollakota, Samuel David Perli, and Dina Katabi. Interference alignment and cancellation. In *Proceedings of the ACM SIGCOMM 2009 conference on Data communication*, pages 159–170, 2009.

[75] Fadel Adib, Swarun Kumar, Omid Aryan, Shyamnath Gollakota, and Dina Katabi. Interference alignment by motion. In *Proceedings of the 19th annual international conference on Mobile computing & networking*, pages 279–290, 2013.

[76] Adriana B Flores, Sadia Quadri, and Edward W Knightly. A scalable multi-user uplink for Wi-Fi. In *13th {USENIX} Symposium on Networked Systems Design and Implementation ({NSDI} 16)*, pages 179–191, 2016.

[77] Wi-Fi spectrum crunch: How to beat slow speeds in crowded areas. https://www.makeuseof.com/tag/wi-fi-spectrum-crunch/.

[78] Hannaneh Barahouei Pasandi, Tamer Nadeem, and Hadi Amirpour. MuViS: Online MU-MIMO grouping for multi-user applications over commodity WiFi. *arXiv preprint arXiv:2106.15262*, 2021.

[79] Sanjib Sur, Ioannis Pefkianakis, Xinyu Zhang, and Kyu-Han Kim. Practical MU-MIMO user selection on 802.11 ac commodity networks. In *Proceedings of the 22nd Annual International Conference on Mobile Computing and Networking*, pages 122–134, 2016.

[80] Shi Su, Wai-Tian Tan, Xiaoqing Zhu, Rob Liston, and Behnaam Aazhang. Data-driven mode and group selection for downlink MU-MIMO with implementation in commodity 802.11 ac network. *IEEE Transactions on Communications*, 69(3):1620–1634, 2021.

8 Appendix

8.1 Generalized N antenna RF virtual chains

Let us consider that the ADC is sampling at NB, and thus we will have N B bandwidth zones obtained from the ADC sampled stream R, denoted by $R_1^B, R_2^B, \ldots R_N^B = \mathbf{R^B}$, with $\mathbf{R^B}$ being a $N \times N_s$ matrix which stores the N_s samples correpsonding to each of the N-th B bandwidth zone, and we can obtain our virtualized RF chains $S_1, S_2, \ldots S_N = \mathbf{S}$, S being $N \times N_s$ as well, via phase inversion of the $N \times N$ phase matrix $\mathbf{P}$ corresponding to the j-th harmonic phase of c_i:

$$\mathbf{S} = (\mathbf{e}^{(-\mathbf{P})}) * \mathbf{R^B} \tag{1}$$

where $\mathbf{e}^{(\cdot)}$ applies the exponential function to each element of the matrix. The matrix $\mathbf{P}$ in detail looks like this:

$$\mathbf{P} = \begin{array}{c} \begin{matrix} 0 & \text{B} & \text{2B} & \ldots & \text{(N-1)B} \end{matrix} \\ \begin{bmatrix} 0 & 0 & 0 & \ldots & 0 \\ 0 & \frac{2\pi}{N} & \frac{4\pi}{N} & \ldots & \frac{2(N-1)\pi}{N} \\ \ldots & \ldots & \ldots & \ldots & \ldots \\ 0 & \frac{2\pi(i-1)}{N} & \frac{4\pi(i-1)}{N} & \ldots & \frac{2(N-1)(i-1)\pi}{N} \\ \ldots & \ldots & \ldots & \ldots & \ldots \\ 0 & \frac{2\pi(N-1)}{N} & \frac{4\pi(N-1)}{N} & \ldots & \frac{2(N-1)(N-1)\pi}{N} \end{bmatrix} \end{array} \begin{matrix} c_1 \\ c_2 \\ \ldots \\ c_i \\ \ldots \\ c_n \end{matrix}$$

8.2 Algorithm to choose maximal set of antennas in-phase

This BABF algorithm chosen $\mathbf{B}$ creates a projected channel $\mathbf{HB}$ such that the remaining interference terms in $\mathbf{HB}$ can be handled easily by digital combining by be inverting this effective channel matrix via ZF approach as, $\mathbf{U} = (\mathbf{HB})^{-1}\mathbf{S}$.

Algorithm 1 BABF, Input: $\mathbf{H}$, Output: $\mathbf{B}$

1: $\phi = \pi/3$;
2: **for** $1 \le i \le K$ **do**
3: **for** $1 \le m \le M$ **do**
4: $\tilde{\mathbf{b}}_{i,m} = [0, 0, \ldots, 0]_{1\times M}$;
5: $\mathbf{g}_{i,m} = \mathbf{H}_i h^*_{i,m}$;
6: $\boldsymbol{\theta}_{i,m} = \angle \mathbf{g}_{i,m}$;
7: $\tilde{\mathbf{b}}_{i,m}(m) = |\boldsymbol{\theta}_{i,m}| < \frac{\pi}{4}$;
8: $score_{i,m}$ = Number of elements equal to 1 in $\tilde{\mathbf{b}}_{i,m}$;
9: **end for**
10: **end for**
11: $\mathbb{B}$:= Set of all possible permutations of $score_{i,m}, 1 \le i \le K, 1 \le m \le M$
12: $l = 1$;
13: Select $score^* \in \mathbb{B}$ that provides the l^{th} highest score;
14: $\mathbf{B} = \mathbf{B}^*$ (corresponding to $score^*$);
15: **if HB** is full rank **then**
16: **B** is the optimal switch configuration;
17: **else**
18: $l = l + 1$;
19: Go to line 13;
20: **end if**